Journal of Plant Protection Research eISSN 1899-007X

ORIGINAL ARTICLE

Identification of a potentially functional *MKS2/ALT* homolog gene in the genome of the cultivated potato *Solanum tuberosum*

Huong Thi Diem Tran, Thuong Thi Hong Nguyen*

Faculty of Biology and Biotechnology, University of Science, Vietnam National University, Ho Chi Minh City, Viet Nam

DOI: 10.24425/jppr.2024.151816

Received: February 03, 2024
Accepted: June 03, 2024
Online publication: February 21, 2025

*Corresponding address:
nththuong@hcmus.edu.vn

Responsible Editor:
Piotr Iwaniuk

Abstract

The Solanaceae family includes many species of plants with high nutritional and medicinal value. Plants in this family have evolved towards diversifying specialized (secondary) metabolism to adapt to adverse conditions, and a few of them have been used as model plants in the study of plant defense. 2-Methylketones are insecticidal compounds that accumulate in certain plants, particularly in wild tomato *Solanum habrochaites* f. *glabratum* – a Solanaceae member. 2-Methylketones are the decarboxylated products of 3-ketoacids generated through the hydrolysis of 3-ketoacyl-ACPs by methylketone synthase 2 (*MKS2*). In this study, we isolated one of the four *MKS2* homolog genes from the cultivated potato *Solanum tuberosum* and designated it as *StMKS2-3*. A combined *in silico* approach including sequence alignment, phylogenetic assessment, 3D structural modeling and RNA-sequencing data analysis was performed to exploit the functional properties of this gene. The encoded protein possesses the conserved Aspartate and functional domain characteristic of single Hotdog-fold thioesterases, and it shares high similarity in sequence and structure with SlMKS2a of the cultivated tomato (*S. lycopersicum*). This suggests that, like SlMKS2a, *StMKS2-3* could act as a 3-ketoacyl-ACP thioesterase. According to RNA-seq data, *StMKS2*-3 exhibited higher expression than the other three *StMKS2* genes in most tissues across different potato *S. tuberosum* cultivars. The quantitative real-time polymerase chain reaction (qRT-PCR) analysis showed that *StMKS2-3* was expressed in multiple potato tissues, both aerial and root parts, but the highest expression was in tubers and sprouts. Furthermore, this gene appeared to be transcriptionally induced in response to salinity, drought, and *Phytophthora infestans* infection, supporting a possible role for *StMKS2-3* in the response of potato *S. tuberosum* to such stress.

Keywords: 3-ketoacyl-ACP thioesterase, 2-methylketone, methylketone synthase 2, *Solanum tuberosum,* stress

Abbreviations:

ACP	acyl carrier protein
ALT	acyl-lipid thioesterase
MKS	methylketone synthase
pLDDT	predicted local distance difference test
TPM	transcripts per kilobase million

Introduction

2-Methylketones are volatile organic compounds that have been synthesized and accumulated in the glandular trichomes of the wild tomato species *Solanum habrochaites* f. *glabratum* (Fridman *et al.* 2005). These compounds could act as biopesticides (Antonious and Snyder 2015; Zhu *et al.* 2018). Specifically, 2-undecanone, 2-dodecanone, 2-tridecanone and 2-pentadecanone are effective in repelling and preventing the two-spotted spider mite (*Tetranychus urticae*) Koch from laying eggs on wild tomato plants (Antonious

and Snyder 2015). 2-Tridecanone causes 100% mortality of the potato aphid (*Macrosiphum euphorbiae*) after 24 hours of exposure (Musetti and Neal 1997). The repellent efficacy of the *Ruta chalepensis* essential oil against the weevil *Aegorhinus superciliosus,* a pest of fruit crops, was largely attributed to high concentrations of 2-nonanone and 2-undecanone in the oil (Tampe *et al.* 2016). The insecticidal and acaricidal activities of 2-methylketones have also been reported on the peach aphid (*Myzus persicae*), the tobacco budworm (*Heliothis virescens*), the corn earworm (*Heliothis zea*), the Colorado potato beetle (*Leptinotarsa decemlineata*), and the sweet potato whitefly (*Bemisia tabaci*) (Antonious *et al.* 2003, 2005).

The molecular mechanism of methylketone biosynthesis in plants was first investigated in the wild tomato *S. habrochaites* with the identification of two genes encoding enzymes that catalyze the last two steps of the pathway, methylketone synthase 1 (*ShMKS1*) and methylketone synthase 2 (*ShMKS2*). While *ShMKS2* hydrolyzes 3-ketoacyl-ACPs, the first intermediates in the fatty acid biosynthesis cycles, into 3-ketoacids, ShMKS1 catalyzes the decarboxylation of the released 3-ketoacids to produce 2-methylketones (Yu *et al.* 2010).

Methylketone synthase 2 (*MKS2*) or acyl-lipid thioesterase (ALT) is a single hot-dog fold thioesterase that has been commonly found in many plant species. When recombinantly expressed in microbial systems such as yeasts, bacteria, etc., all plant MKS2/ALTs exhibited 3-ketoacyl-ACP thioesterase activity, with variations in the composition and proportion of the β-ketoacid products. *E. coli* BL21(DE3) cells expressing *ShMKS2* could synthesize β-ketoacids which are subsequently reduced to the odd-chain 2-methylketones, including 2-undecanone (11:0), 2-tridecanone (13:0) and 2-pentadecanone (15:0). Out of these, 2-tridecanone (13:0) is the main product. Although SlMKS2a from the cultivated tomato *Solanum lycopersicum* shares more than 90% sequence similarity with *ShMKS2*, it catalyzes the synthesis of β-ketoacids that are precursors of 2-nonanone (9 : 0), 2-undecanone (11 : 0), 2-tridecanone (13 : 0) and 2-tridecenone (13 : 1), among which 2-tridecenone (13 : 1) is the most abundant (Ben-Israel *et al.* 2009). Moreover, eggplant *Solanum melongena* (Sm), another member of the Solanaceae family, also possesses two functional *MKS2* genes, *SmMKS2-1* and *SmMKS2-2*. *SmMKS2-1* participates in the synthesis of saturated 2-methylketones with carbon skeletons ranging from 7C to 17C and monounsaturated 2-methylketones with carbon skeletons in the range of 13C–17C. *SmMKS2-2* is involved in the formation of mainly 2-tridecenone (13 : 1) and smaller amounts of saturated 2-methylketones 9 : 0, 11 : 0 and 13 : 0 as well as unsaturated 2-methylketones 11 : 1 and 15 : 1 (Khuat *et al.* 2019).

The Solanaceae family includes many species of plants with high nutritional and medicinal value. Plants in this family have evolved towards diversifying specialized (secondary) metabolism to adapt to adverse conditions. Typically, the wild tomato species *S. habrochaites* has long been known for its resistance to a wide range of pests and pathogens, thanks to its production of medium-chain 2-methylketones in trichomes (Maluf *et al.* 1997). In contrast, cultivated tomato (*S. lycopersicum*) plants contain little or no methylketones. When exposed to biotic or abiotic stresses, one of the most common responses of plants is the induction of biosynthesis of specialized compounds through stimulating the expression of genes encoding enzymes in the biosynthetic pathway (Isah 2019). It has been shown that eggplant (*S. melongena*) possesses one *MKS2* homolog gene (namely *SmMKS2-1*) that is transcriptionally upregulated in leaves by stress signals such as mechanical wounding, methyl jasmonate (MeJA), or methyl salicylate (MeSA). Potato (*Solanum tuberosum*) is another important representative of the Solanaceae family, and it is the world's fourth largest food crop after wheat, rice and maize (Gebrechristos and Chen 2018). Potatoes are sensitive and vulnerable to a wide range of environmental stresses such as cold, drought, salinity and attack by pathogens and pests, leading to significant yield loss (Cwalina-Ambroziak *et al.* 2015; Lenc *et al.* 2016; Tiwari *et al.* 2022). To achieve sustainable potato production, it is necessary to explore the physiological, biochemical, and molecular mechanisms underlying the resistance and tolerance of potatoes to various types of stress (Fatima *et al.* 2019). A functional understanding of genes regulated by stress signals could enable scientists to formulate strategies to make potatoes better adapt to their environment.

The genome sequence of *S. tuberosum* group Phureja DM1–3 516 R44 was first published in 2011 using whole-genome shotgun (WGS) sequencing approach, and updated in 2020 using Oxford Nanopore sequencing technology coupled with proximity ligation scaffolding (Xu *et al.* 2011; Pham *et al.* 2020). The availability of current advanced sequencing technologies permitted generation of a high-quality chromosome-scale assembly of the potato reference genome. In addition, full-length complementary DNA (cDNA) sequencing using Oxford Nanopore Technologies (ONT) made significant improvements in the accuracy and completeness of gene model annotations compared to previous prediction results (Pham *et al.* 2020). This paves the way for research on improving the agronomic traits and understanding genome evolution of potatoes.

In this study, we report the finding of four *MKS2* homolog gene models in the potato genome, and further validate their presence by RNA-seq data. We

obtained a full-length transcript for one of four putative *MKS2 g*enes, namely *StMKS2-3*, from mixed tissues of the cultivated potato *S. tuberosum*. Quantitative real-time polymerase chain reaction (qRT-PCR) analysis and *in silico* investigation including sequence alignment, phylogenetic assessment, 3D structural modeling and RNA-sequencing data processing were performed to exploit the functional properties of this gene.

Materials and Methods

Plant materials

Potato plants (*Solanum tuberosum*) were grown in a screenhouse erected at the field station of the Potato Vegetable and Flower Research Center (Lam Dong, Vietnam), with average temperatures ranging from 14°C to 27°C. The soil was supplemented with cococoir to help with aeration and water retention and was watered to the moisture content of 80% about 2 days before being used for planting. Samples collected from these plants were used for gene isolation by PCR and gene expression analysis by qRT-PCR.

Identification of *MKS2* model genes in potato *Solanum tuberosum* using bioinformatics tools

ShMKS2 protein sequence (Genbank accession: ADK38536.1) was used as a query sequence for TBLASTN searches of "*S. tuberosum* group Phureja DM 1–3 516 R44 high confidence gene models – cDNA (v6.1)" dataset in the Spud database (Spud DB – Potato Genomics Resource: http://spuddb.uga.edu/blast.shtml) to identify *MKS2* homolog genes in potato (*StMKS2*). The exon-intron structure of the *StMKS2* genes was predicted using the FGENESH gene finder program (www.softberry.com) and manually curated based on the alignment to the known homologous cDNA sequences.

RNA-seq data analysis

Gene expression values (transcripts per kilobase million – TPM) for 219 RNA-seq libraries of *S. tuberosum* from the Sequence Read Archive (SRA) were generated using Kallisto (v0.46.2) (Hamilton *et al.* 2011; Massa *et al.* 2011; Felcher *et al.* 2012). RNA-seq data from different potato cultivars were downloaded from the Spud DB and used to analyze the transcriptional expression pattern of *StMKS2* genes across tissues of *S. tuberosum* and under stress conditions. Expression profiles of *StMKS2* genes were visualized as heatmaps using Heatmap Illustrator 2.0 (http://hemi.biocuckoo.cn/).

Isolation of *StMKS2-3* CDS

Equal amounts of various tissues including shoot apex, stem, and young tuber of potato plants grown at the Potato Vegetable and Flower Research Center (Lam Dong, Vietnam) were collected and mixed. The total RNA was extracted from this potato tissue mixture using the EZ-10 Spin Column Plant RNA Mini-Prep kit (Bio Basic Inc., Ontario, Canada), treated with DNase I to remove genomic DNA contamination, and converted to cDNA using RevertAid First Strand cDNA Synthesis kit (Thermo Fisher Scientific, Massachusetts, USA). The coding sequence of *StMKS2-3* (*StMKS2-3* CDS) was amplified from cDNA by PCR using gene-specific primers (forward primer *StMKS2-3*-F: GAATTCATGTCTCAGTCCCTCGCT; reverse primer *StMKS2-3*-R: GGATCCTGTTAGATGCCTCCTGG). PCR reactions were set up with the following components: 1 µl of cDNA, 0.4 µl of 10 mM dNTP mix, 4 µl of 5X Phusion HF buffer, 0.2 µl of Phusion High-Fidelity DNA polymerase, 0.4 µl of 10 mM for each of the two primers, and DNase-free distilled water to the total volume of 20 µl. Thermal cycling conditions for PCR consisted of an initial denaturation at 98°C for 30 s, 35 cycles of 98°C for 10 s, 58°C for 20 s, and 72°C for 20 s, and a final extension at 72°C for 10 min.

The PCR product was examined by agarose gel electrophoresis. The expected product was purified using the GeneJET Gel Extraction kit (Thermo Fisher Scientific, Massachusetts, USA) according to the manufacturer's instructions and cloned into the pJET1.2/blunt vector. The recombinant plasmid was transformed into *E. coli* TOP10 competent cells. The *E. coli* TOP10/pJET1.2-*StMKS2-3* transformants were screened by colony PCR using gene-specific forward primer (*StMKS2-3*-F) and vector-specific reverse primer (pJET1.2-R: AAGAACATCGATTTTCCATGGCAG). Thermal cycling was 95°C for 30 s, 35 × (95°C for 50 s, 58°C for 20 s, 72°C for 40 s), and 72°C for 5 min. The recombinant plasmid was extracted using the GeneJET Plasmid Miniprep kit and the integrity of the insert was verified by sequencing. The *StMKS2-3* CDS sequence was deposited in GenBank with accession number PP236921.

Phylogenetic analysis of the *StMKS2-3*

The amino acid sequences of *StMKS2-3* and homologous proteins from *Arabidopsis thaliana,* soybean *Glycine max* and several Solanaceae species including wild tomato *Solanum habrochaites*, cultivated tomato *Solanum lycopersicum*, eggplant *Solanum melongena,* tobacco *Nicotiana tabacum,* and pepper *Capsicum annuum* were aligned by MUSCLE v3.8.31 (Edgar 2004) and the maximum-likelihood phylogenetic tree was inferred by IQ-TREE 1.5.5 (Nguyen *et al.* 2015).

Analysis of *StMKS2-3* protein structure

The presence of conserved structural domains of *StMKS2-3* protein was predicted by Interpro (Paysan-Lafosse *et al.* 2023). The 3D structure of *StMKS2-3* was predicted by Alphafold2 on Google Colab (Mirdita *et al.* 2022). Structural superimposition and comparison between two proteins were performed in UCSF ChimeraX using Matchmaker (Pettersen *et al.* 2021).

Gene expression analysis by quantitative real-time polymerase chain reaction (qRT-PCR)

Total RNA was separately isolated from various tissues (root, stem, tuber, young leaf, mature leaf, petiole, and sprout) of 2.5-month-old *S. tuberosum* plants using the EZ-10 Spin column Plant RNA Mini-preps Kit (Bio Basic Inc., Ontario, Canada). The isolated RNA was treated with RNase-free DNase I (Thermo Scientific, Massachusetts, USA) to remove contaminated genomic DNA. The integrity of the extracted RNA was assessed by agarose gel electrophoresis. cDNA was synthesized from 0.5 µg of DNase-free total RNA in a 20-µl reaction using RevertAid First Strand cDNA Synthesis Kit (Thermo Scientific, Massachusetts, USA) and oligo $(dT)_{18}$ primer. Gene-specific primers were designed using OligoAnalyzer 3.1 (Integrated DNA Technologies, Inc., Iowa, USA) and Primer-BLAST program provided by the National Center for Biotechnology Information (NCBI) (Supplementary File 1). One ul of cDNA diluted 10 times was subjected to each of 10-ul quantitative real-time polymerase chain reactions (qRT-PCR) containing 1X SolGent *h-Taq* Reaction Buffer, 1X Eva-Green™ Dye (Biotium, California, USA), 1 mM $MgCl_2$, 0.2 mM dNTP, 0.025 U · µl^{-1} SolGent™ *h-Taq* polymerase (SolGent, Daejeon, Korea), and 400 nM of each primer (Supplementary File 1). Thermal cycling conditions were set up in a Lightcycler 96 system (Roche, Basel, Switzerland) with one cycle at 95°C for 15 min, followed by 40 cycles of 95°C for 20 s, 62°C for 40 s, and 72°C for 8 s. The expression levels of the *StMKS2-3* gene were normalized to those of the reference gene *StRPL19* (GenBank: XM_006355756.2) and expressed as relative expression (Li *et al.* 2020). Each data point represents an average of at least three independent biological samples with three technical replicates for each.

Results

Identification of *StMKS2* gene models

TBLASTN search against Spud database (Spud DB – Potato Genomics Resource: http://spuddb.uga.edu/blast.shtml) using *ShMKS2* as a query sequence identified four gene models encoding polypeptides with homology to the *ShMKS2* protein (Table 1). Based on the homology to *ShMKS2* and other homologous sequences from *Arabidopsis thaliana* and Solanaceae species, the exon-intron structure of *StMKS2* genes was predicted as shown in Figure 1 and Supplementary File 2.

The *StMKS2* genes are structurally similar to many other characterized plant *MKS2* genes, with 5 exons and 4 introns. The coding sequence (CDS) regions of four putative *StMKS2* genes, including *StMKS2-1*, *StMKS2-2*, *StMKS2-3* and *StMKS2-4*, have predicted sizes of 633, 630, 627 and 627 bp, respectively.

Transcriptional expression pattern of *StMKS2* genes according to RNA-seq data

The RNA-seq data collected from many tissues of different *S. tuberosum* cultivars (RH89-039-16, Phujera, Superior, DM1-3 516 R44, Atlantic, Premier Russet and Snowden) and archived in the publicly accessible Spud database were used for generating the spatial expression pattern of the *StMKS2* genes (Fig. 2). Accordingly, *StMKS2*-1 transcripts were found in one or several of the following tissues: tuber, shoot apex, leaf, root, stolon, and flowers, depending on the cultivar. Generally, this gene showed medium and low

Table 1. Gene models encoding polypeptides with homology to the ShMKS2 protein collected from Spud database

No.	Accession number	Identity [%]	E-value	Name
1	Soltu.DM.04G001960.1	87.75	1e-132	*StMKS2-1*
2	Soltu.DM.04G001980.1	81.82	1e-126	*StMKS2-2*
3	Soltu.DM.04G002110.1	74.61	1e-101	*StMKS2-3*
4	Soltu.DM.04G001990.1	78.17	1e-81	*StMKS2-4*

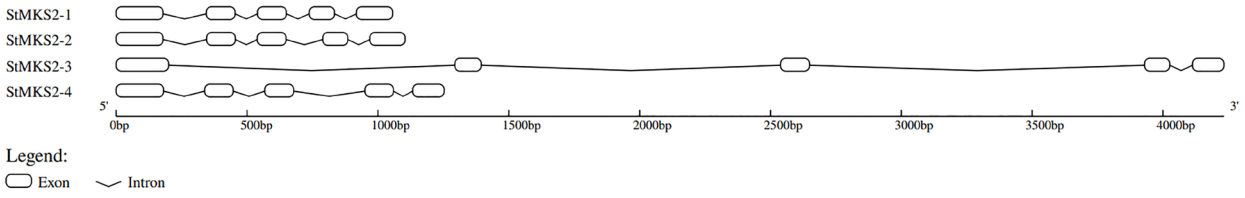

Fig. 1. Exon-intron structures of the putative *StMKS2* genes. Exons are represented as boxes, and introns are represented as lines

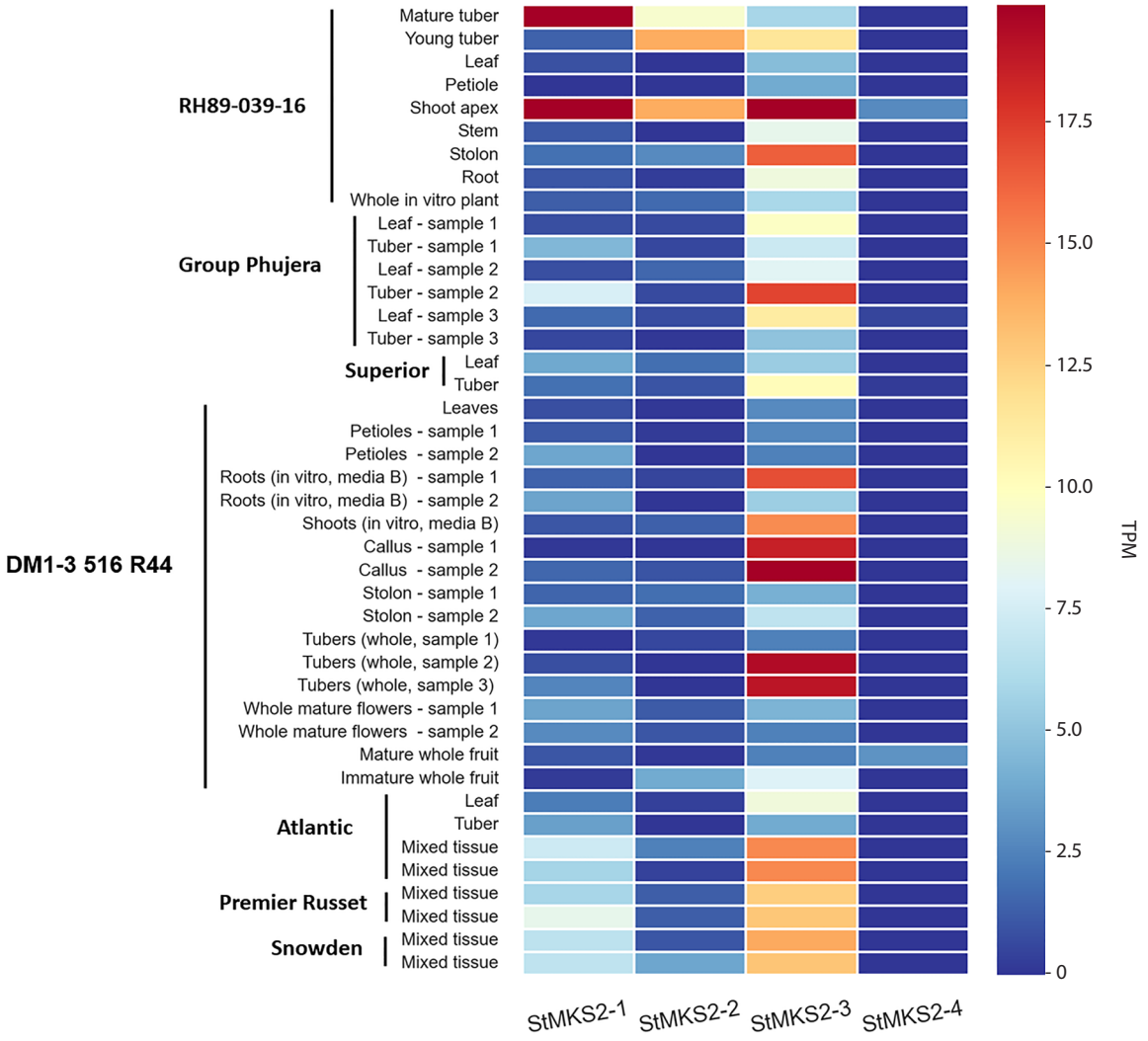

Fig. 2. Heatmap of RNA-seq based expression data of *StMKS2* genes in different tissues of various *S. tuberosum* cultivars

expression levels (TPM < 10) in most of the tested tissues except in mature tuber and shoot apex of the heterozygous diploid potato (RH89-039-16) with TPM > 17.5. Similarly, *StMKS2-2* transcripts were mostly present in the tuber and shoot apex of *S. tuberosum* cultivar RH89-039-16. In contrast, *StMKS2-3* was expressed in all tissues examined, with expression levels varying across tissue types and cultivars. *StMKS2-4* transcripts were not found in most tissues, except for being detected at low levels (TPM < 5) in the shoot apex of cultivar RH89-039-16 and the mature fruit of cultivar DM1-3 516 R44.

RNA-seq data obtained from mixed tissues of *S. tuberosum* cultivar Atlantic, Premier Russet or Snowden also showed that *StMKS2-3* had the highest expression level, followed by *StMKS2-1* and then *StMKS2*-2. Meanwhile, *StMKS2-4* was not expressed in these cultivars.

In summary, the results obtained from RNA-seq data showed that *StMKS2-3* might express at a higher level than the other three *StMKS2* genes in many tissues across different cultivars of *S. tuberosum* (RH89-039-16, Phujera, Superior, DM1-3 516 R44, Atlantic, Premier Russet and Snowden). For this reason, *StMKS2-3* is believed to have important biological functions in potato plants and was thus selected for isolation and functional analysis.

Isolation of the coding sequence of the *StMKS2-3* gene from *Solanum tuberosum*

The coding region of the *StMKS2-3* gene was amplified by PCR using cDNA prepared from a mixture of *S. tuberosum* tissues as a template and a pair of primers specific to the beginning and the end of the predicted sequence of the gene. The electrophoretic result of the PCR product showed that there was a band with a size equivalent to the predicted size of *StMKS2-3* CDS (627 bp) in lane 1 where the amplified product from cDNA of *S. tuberosum* was loaded. By contrast, the band of the same size was absent from lane 3 where the PCR product of no template control was loaded (Fig. 3).

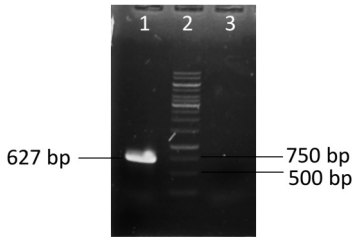

Fig. 3. PCR amplification of the entire coding sequence of *StMKS2-3* using cDNA template prepared from a mixture of *S. tuberosum* tissues. 1 – PCR product of *StMKS2-3* CDS; 2 – 1 kb DNA ladder; 3 – negative (no template) control

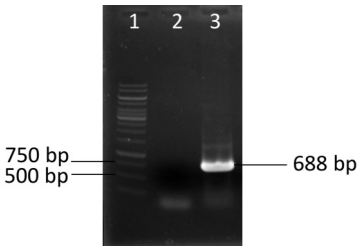

Fig. 4. Screening *Escherichia coli* TOP10 clones carrying the recombinant plasmid (pJET1.2-*StMKS2-3*) by colony PCR. 1 – negative (no template) control; 2 – 1 kb DNA ladder; 3 – colony PCR product of one randomly chosen clone using *StMKS2-3*-F and pJET1.2-R primers

The specific PCR product was purified and inserted into the pJET1.2/blunt vector. The result of PCR screening of *E. coli* TOP10 colonies carrying the plasmid pJET1.2-*StMKS2-3* was shown in Figure 4. A band with a size corresponding to the expected size of the colony PCR product of a clone carrying the plasmid pJET1.*2-StMKS2-3* was observed in lane 3 of the agarose gel. By contrast, the negative (no template) control in lane 1 did not show this band. This result suggests that the colony used as DNA template in lane 3 (Fig. 4) is possibly the one carrying the recombinant plasmid pJET1.2-*StMKS2*-3. The plasmid was extracted from this putative *E. coli* TOP10/pJET1.2-*StMKS2*-3 transformant and sequenced with the vector-specific primer (pJET1.2-F) to verify the integrity of the inserted DNA fragment.

The isolated *StMKS2-3* CDS was 99.36% identical to the predicted sequence, with four different nucleotides at positions 287, 429, 435, 465 from the initiating codon ATG (Supplementary File 3). The protein sequence deduced from the *StMKS2-3* CDS contains 208 amino acids and differs only by one amino acid at position 96 from the predicted protein (Supplementary File 4).

StMKS2-3 contains a signal peptide sequence at its N-terminus and has all the characteristics of a single Hotdog-fold thioesterase

All known functional *MKS2/ALT* thioesterases in plants possess a single "Hotdog" domain (Yu *et al.* 2010; Pulsifer *et al.* 2014; Tran *et al.* 2019). In this study, Interpro analysis showed that *StMKS2-3* has a complete Hotdog domain spanning from amino acids 86 to 169 (Interpro: IPR006683) (Supplementary File 5) (Paysan-Lafosse *et al.* 2023). In addition, amino acid sequence alignment between *StMKS2-3* and other functionally characterized homologs from *Pseudomonas* sp, *Arabidopsis thaliana*, and plant species of the Solanaceae family showed that *StMKS2-3* also contains the conserved aspartate necessary for the catalytic activity of single "Hotdog" thioesterases (Fig. 5).

According to the protein sequence alignment results (Fig. 5), Met^{68} of *StMKS2-3* aligns with the first amino acid of the known mature *MKS2/ALT* proteins. This suggests that Met^{68} can be the initial amino acid of mature *StMKS2-3* (*mStMKS2-3*) and the N-terminal 67-amino acid sequence preceding this residue might act as a signal peptide to target the *StMKS2-3* protein to the chloroplast, as observed in other plant MKS2/ALT proteins (Yu *et al.* 2010; Pulsifer *et al.* 2014).

StMKS2-3 has a strong sequence and structural similarity to SlMKS2a

The phylogenetic tree inferred from the amino acid sequence alignment of *StMKS2-3* and homologous thioesterases from *Pseudomonas* sp, *Arabidopsis thaliana*, *Glycine max*, and Solanaceae species was shown in Figure 6. Among functionally characterized thioesterases included in the analysis, SlMKS2a of the cultivated tomato *S. lycopersicum* showed the highest sequence similarity to *StMKS2*-3 (98%) (Yu *et al.* 2010). Consequently, *StMKS2-3* and SlMKS2a are clustered on the same branch of the phylogenetic tree (Fig. 6).

Protein structure determines its biological function. Two proteins with similar structures will often have similar functions (Anfinsen 1973). Prediction and comparison of protein structures therefore can aid in understanding protein functions. AlphaFold is an artificial intelligence software capable of predicting a protein structure based on its sequence with a level of accuracy equivalent to that of the experimentally determined structures (Jumper *et al.* 2021). The three-dimensional (3D) structure model of *StMKS2-3* predicted by Alphafold 2 is colored according to the pLDDT (predicted local distance difference test) values (Fig. 7A). Except for the first three amino acids at the N-terminus and the last 10 amino acids at the C-terminus with pLDDT between 50 and 70, roughly 90% of the residues across the predicted

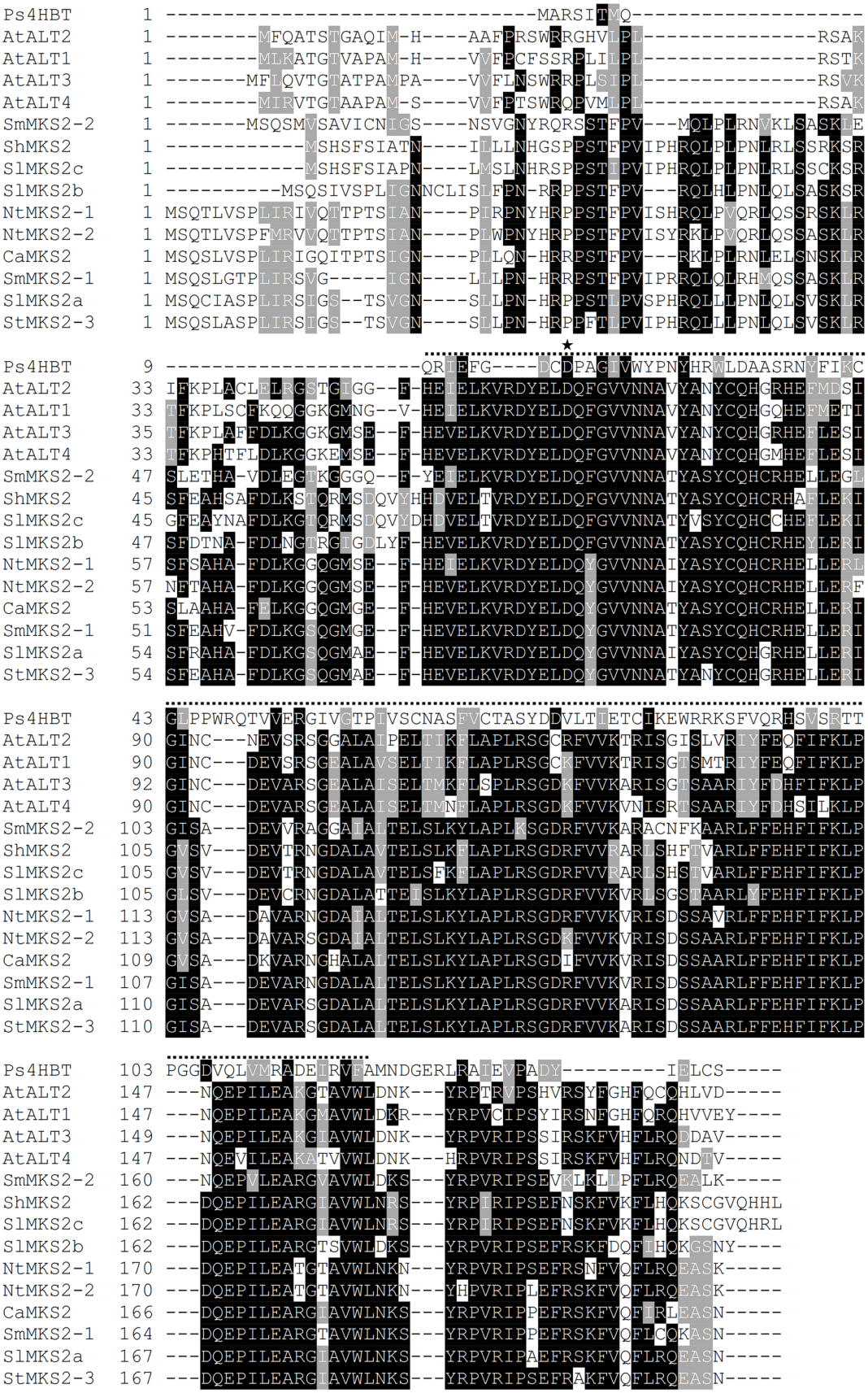

Fig. 5. Amino acid sequence alignment of *StMKS2-3* and functionally characterized homologous proteins from *Pseudomonas* sp., *Arabidopsis thaliana*, and selected Solanaceae plants. Dashed line indicates the conserved Hotdog-fold region. The star represents the conserved Asp residue. Accession numbers are as follows: AtALT1 (AEE31776.1), AtALT2 (AEE31773.1), AtALT3 (AEE34774.1), AtALT4 (AEE34776.2), CaMKS2, GmMKS2-X2 (QFR04503.1), NtMKS2-1, NtMKS2-2, Ps4HBT (EF569604), *ShMKS2* (ADK38536.1), SlMKS2a (ADK38541.1), SlMKS2b (ADK38542.1), SlMKS2c (ADK38543.1), *SmMKS2-1* (QDV39734.1), and *SmMKS2-2* (QDV39735.1)

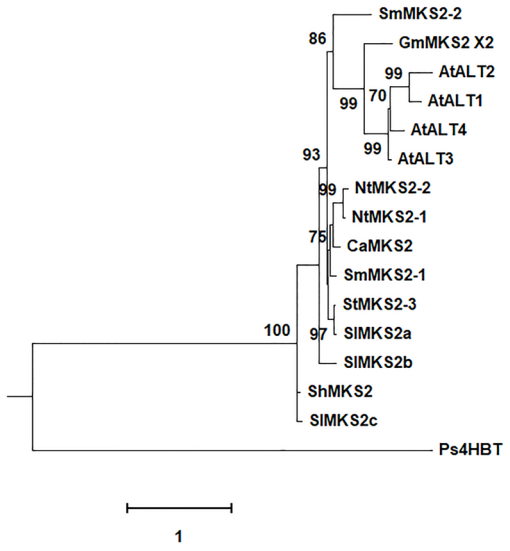

Fig. 6. Maximum likelihood phylogenetic tree of *StMKS2-3* and selected functionally characterized plant MKS2/ALTs. The numbers close to nodes represent bootstrap values, which were obtained from 1000 replicates and reported as percentages

structure of *StMKS2-3*, including the conserved aspartate (D17, Fig. 7) and those in the Hotdog domain, have an average high (70 < pLDDT < 90) to very high (pLDDT > 90) confidence (Fig. 7A).

Searching for proteins with predicted structures similar to that of *StMKS2*-3 in three databases including Protein Structure Sequences, AlphaFold DB and UniprotKB PDB identified SlMKS2a (AFDB: B5B3P5) as the protein with the highest structural similarity to *StMKS2-3* (Supplementary File 6). The RMSD values calculated from superposition of the Alphafold model of *StMKS2-3* with the structure of SlMKS2a (AFDB: B5B3P5) were 0.281 Å (Fig. 7B). This RMSD value falls in the recommended range of 0–2 Å, indicating that the StMKS2-3 model is very similar to the SlMKS2a structure (Carugo and Pongor 2001).

Expression analysis of *StMKS2-3* in different organs or parts of potato plants by qRT-PCR

A search of the publicly available RNA-seq data downloaded from the Spud DB revealed that *StMKS2-3* was expressed in all tissues examined, with expression levels varying across tissue types and cultivars (Fig. 2). To validate the expression pattern of *StMKS2-3* obtained from transcriptome sequencing data, in this study, we measured the relative transcriptional expression of this gene in different tissues of *S. tuberosum* plants by qRT-PCR. The results showed that transcripts of *StMKS2-3* were detected to varying levels in all the organs or parts tested (root, stem, tuber, young leaf, mature leaf, petiole, and sprout). Specifically, the expression of *StMKS2-3* was highest in tubers and sprouts, much lower in roots and petioles, and the lowest in stems and leaves (Fig. 8). The expression pattern of *StMKS2*-3 detected by qRT-PCR was highly correlated with that obtained from RNA-seq based analysis of respective tissues of two potato cultivars (RH89-039-16 and DM1-3 516 R44) where the target transcripts were most abundant in the tuber or shoot apex. For five other remaining cultivars (Phujera, Superior, Atlantic, Premier Russet and Snowden), only RNA-seq data collected from tubers, leaves, and/or mixed tissues were available in the Spud DB.

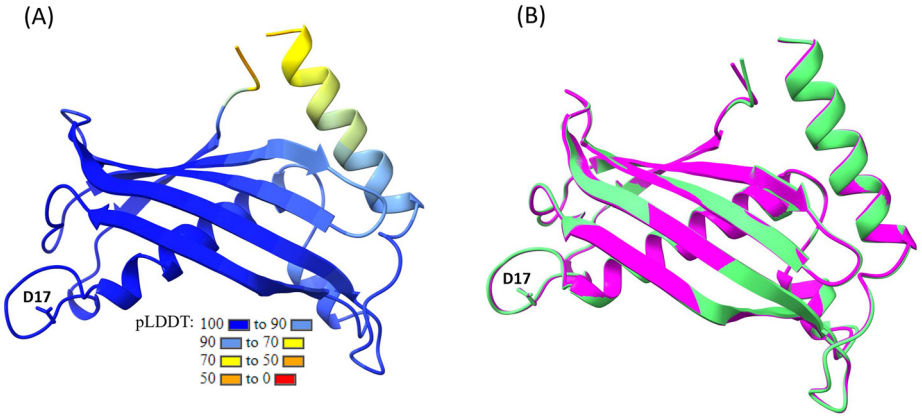

Fig. 7. 3D structure model of *StMKS2-3* predicted by Alphafold2 – A and structural similarity between *StMKS2-3* and *SlMKS2a* – B. A, The Alphafold2 predicted model of *StMKS2*-3 is colored according to the pLDDT values. pLDDT > 90: very high confidence; 70 < pLDDT < 90: high confidence; 50 < pLDDT < 70: low confidence; pLDDT < 50: very low confidence; B, Superimposition of the Alphafold2 predicted structure of *StMKS2-3* (pink) to the structural model of SlMKS2a deposited in the Alphafold database (AFDB:B5B3P5) (green). The root mean square deviation (RMSD) between 141 atom pairs is 0.281 Å. "D17" corresponds to the conserved aspartate

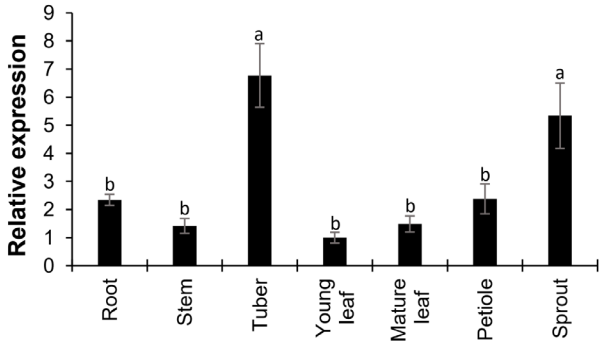

Fig. 8. Relative expression levels of *StMKS2-3* transcripts in different organs or parts of *S. tuberosum*, determined by qRT-PCR. Expression values were normalized to those of *StRPL19* (Genbank accession: XM_006355756.2). Each value is the mean ± standard error (SE) from three biological replicates. Significant differences were assessed by one-way ANOVA followed by Tukey's HSD test. Bars with different letters are significantly different ($p < 0.05$)

Discussion

StMKS2-3 is a potentially functional *MKS2/ALT* in potato *Solanum tuberosum*

Amino acid sequence alignment between *StMKS2-3* and other functionally characterized homologs from *Pseudomonas* sp, *Arabidopsis thaliana*, and plant species of the Solanaceae family showed that *StMKS2-3* contains all the characteristics of a single Hotdog-fold thioesterase including a Hotdog domain spanning from amino acids 86 to 169 (Interpro: IPR006683) and a conserved aspartate necessary for the catalytic activity of a typical single "Hotdog" thioesterase (Fig. 5 and Supplementary File 5). The amino acid sequence of *StMKS2-3* showed the highest similarity with that of SlMKS2a from the cultivated tomato *S. lycopersicum* (98% identity; accession no. NP_001334492.1) (Yu *et al.* 2010). In line with this, searching for proteins with predicted structures similar to that of StMKS2-3 in three databases including Protein Structure Sequences, AlphaFold DB and UniprotKB PDB also identified SlMKS2a (AFDB: B5B3P5) as the protein with the highest structural similarity to *StMKS2-3* (Supplementary File 6). It has been shown that SlMKS2a exhibits 3-ketoacyl-ACP thioesterase activity when recombinantly expressed in *E. coli* (Ben-Israel *et al.* 2009). Specifically, SlMKS2a hydrolyzes a range of medium-chain 3-ketoacyl-ACPs (10–14 C) to 3-ketoacids (or β-ketoacids), which can be readily decarboxylated to the corresponding 2-methylketones (Kornberg *et al.* 1948; Yu *et al.* 2010). The homology in sequence and structure between two proteins suggests that *StMKS2-3* might have a similar catalytic activity to SlMKS2a. Our qRT-PCR analysis showed that this gene is expressed in multiple tissues at different developmental stages. In other words, potatoes possess at least one potential functional MKS2/ALT, and an *in vitro* enzymatic characterization of this protein would give more confirmative conclusion.

StMKS2-3 might have an important role in the stress responses of *Solanum tuberosum*

Following the first discovery of *ShMKS2* from the wild tomato *S. habrochaites*, *ShMKS2* homologs have been found in a wide range of plant species (Pulsifer *et al.* 2014; Kalinger *et al.* 2018; Khuat *et al.* 2019; Tran *et al.* 2019). Although the *in planta* biological function of MKS2/ALT-like proteins awaits further investigation, there is collective evidence that supports a defensive role for these thioesterases in many plant species (Ben-Israel *et al.* 2009; Pulsifer *et al.* 2014; López-Lara *et al.* 2018; Khuat *et al.* 2019). *MKS2s/ALTs* primarily catalyze the hydrolysis of 3-ketoacyl-ACP intermediates of the fatty acid biosynthetic pathway into corresponding 3-keto fatty acids, which are subsequently decarboxylated to the odd-chain 2-methylketones (Yu *et al.* 2010). The 2-methylketone products, especially medium-chain MKs such as 2-undecanone (11 : 0) and 2-tridecanone (13 : 0), are secondary compounds that abundantly accumulate in the secretory glandular trichomes of the wild tomato *S. habrochaites* (Ben-Israel *et al.* 2009) and have been shown to have insecticidal activity (Kennedy *et al.* 1981; Antonious *et al.* 2003; Antonious 2004; Antonious and Snyder 2006). The eggplant *Solanum melongena*, another representative of the Solanaceae family, possesses two functional *MKS2/ALT* genes, one of which is transcriptionally upregulated following artificial wounding, methyl jasmonate (MeJA) treatment, or methyl salicylate (MeSA) treatment (Khuat *et al.* 2019). It has also been reported that herbivore-damaged Arabidopsis plants emitted significantly higher amounts of 2-pentanone than undamaged plants (van Poecke *et al.* 2001). Recently, a new role has been assigned to 2-tridecanone as an infochemical that affects surface mobility and biofilm formation in plant pathogenic bacteria and thus interferes with microbial colonization of plant tissues (López-Lara *et al.* 2018). In this study, our analysis of RNA-seq data showed that the level of *StMKS2-3* transcripts appears to be increased following 24 h treatment with 150 mM NaCl or 260 μM mannitol, and 1–2 days after *Phytophthora infestans* infection (Supplementary File 7). NaCl and mannitol are often added to the medium at high concentrations to simulate salinity and drought stress conditions, respectively (Sattar *et al.* 2021), while *P. infestans* is the causative agent of late blight that results in potato yield loss (Dong

and Zhou 2022). Transcriptional induction of the *StMKS2-3* gene by 150 mM NaCl, 260 μM mannitol and the fungus *P. infestans* provides the first experimental evidence-based hint of the possible involvement of this gene in the response of *S. tuberosum* to salinity, drought and phytopathogenic attack. Furthermore, qRT-PCR analysis showed that *StMKS2-3* transcripts were expressed in multiple potato tissues, both aerial and root parts, but were highest in tubers and sprouts, suggesting that *StMKS2-3* may be involved in more than one biological function in potatoes.

Conclusions

In this study, in the genome of potato *S. tuberosum* we identified four *MKS2* homolog gene models, the existence of which is validated by RNA-seq data. Compared to the three remaining *StMKS2* genes, *StMKS2-3* is abundantly expressed in many tissues of various *S. tuberosum* cultivars. The entire coding sequence of *StMKS2-3* obtained from mixed tissues of *S. tuberosum* is 627 bp in size and encodes a polypeptide of 23.4 kDa. *StMKS2-3* possesses the conserved aspartate as well as the functional domain characteristic of single Hotdog-fold thioesterases, and it shares a great similarity in terms of sequence and structure to SlMKS2a of the cultivated *S. lycopersicum,* which implies that *StMKS2-3* has a similar catalytic function as SlMKS2a. Furthermore, *StMKS2-3* is expressed at the highest levels in tubers and sprouts, and its transcriptional expression appears to be upregulated by salinity (150 mM NaCl), drought (260 μM mannitol), and *P. infestans* infection, suggesting a possible role of *StMKS2-3* in the response of potato *S. tuberosum* to such stress.

Acknowledgements

This research was funded by the University of Science, VNU-HCM under grant number T2021-18. The authors acknowledge Dr. Nhuan The Nguyen from the Potato Vegetable and Flower Research Center (Lam Dong, Vietnam) for providing us with the raw materials to conduct this study.

References

Anfinsen C.B. 1973. Principles that govern the folding of protein chains. Science 181 (4096): 223–230. DOI: https://doi.org/10.1126/science.181.4096.223

Antonious G.F. 2004. Persistence of 2-tridecanone on the leaves of seven vegetables. Bulletin of Environmental Contamination and Toxicology 73 (6): 1086–1093. DOI: https://doi.org/10.1007/s00128-004-0536-4

Antonious G.F., Dahlman D.L., Hawkins L.M. 2003. Insecticidal and acaricidal performance of methyl ketones in wild tomato leaves. Bulletin of Environmental Contamination and Toxicology 71 (2): 400–407. DOI: https://doi.org/10.1007/s00128-003-0178-y

Antonious G.F., Kochhar T.S., Simmons A.M. 2005. Natural products: Seasonal variation in trichome counts and contents in *Lycopersicum hirsutum* f. *glabratum*. Journal of Environmental Science and Health – Part B Pesticides, Food Contaminants, and Agricultural Wastes 40 (4): 619–631. DOI: https://doi.org/10.1081/PFC-200061567

Antonious G.F., Snyder J.C. 2006. Natural products: Repellency and toxicity of wild tomato leaf extracts to the two-spotted spider Mite, Tetranychus urticae Koch. Journal of Environmental Science and Health – Part B Pesticides, Food Contaminants, and Agricultural Wastes 41 (1): 43–55. DOI: https://doi.org/10.1080/03601230500234893

Antonious G.F., Snyder J.C. 2015. Repellency and oviposition deterrence of wild tomato leaf extracts to spider mites, Tetranychus urticae Koch. Journal of Environmental Science and Health. Part. B, Pesticides, Food Contaminants, and Agricultural Wastes. 50 (9): 667–673. DOI: https://doi.org/10.1080/03601234.2015.1038960

Ben-Israel I., Yu G., Austin M.B.B., Bhuiyan N., Auldridge M., Nguyen T., Schauvinhold I., Noel J.P.P., Pichersky E., Fridman E. 2009. Multiple biochemical and morphological factors underlie the production of methylketones in tomato trichomes. Plant Physiology 151 (4): 1952–1964. DOI: https://doi.org/10.1104/pp.109.146415

Carugo O., Pongor S. 2001. A normalized root-mean-square distance for comparing protein three-dimensional structures. Protein Science 10 (7): 1470–1473. DOI: https://doi.org/10.1110/ps.690101

Cwalina-Ambroziak B., Damszel M.M., Głosek-Sobieraj M. 2015. The effect of biological and chemical control agents on the health status of the very early potato cultivar Rosara. Journal of Plant Protection Research 55 (4): 389–395. DOI: https://doi.org/10.1515/jppr-2015-0052

Dong S., Zhou S. 2022. Potato late blight caused by *Phytophthora infestans*: From molecular interactions to integrated management strategies. Journal of Integrative Agriculture 21 (12): 3456–3466. DOI: https://doi.org/10.1016/j.jia.2022.08.060

Edgar R.C. 2004. MUSCLE: a multiple sequence alignment method with reduced time and space complexity. BMC Bioinformatics 5 (6): 113. DOI: https://doi.org/10.1186/1471-2105-5-113

Fatima N., Tabassum B., Yousaf I., Malik M., Toufiq N., Sajid I.A., Riaz S., Nasir I.A. 2019. Potential of endochitinase gene to control Fusarium wilt and early blight disease in transgenic potato lines. Journal of Plant Protection Research 59 (3): 376–382. DOI: https://doi.org/10.24425/jppr.2019.129755

Felcher K.J., Coombs J.J., Massa A.N., Hansey C.N., Hamilton J.P., Veilleux R.E., Buell C.R., Douches D.S. 2012. Integration of two diploid potato linkage maps with the potato genome sequence. Aerts, J., ed. PLoS ONE. 7 (4): e36347 DOI: https://doi.org/10.1371/journal.pone.0036347

Fridman E., Wang J., Iijima Y., Froehlich J.E., Gang D.R., Ohlrogge J., Pichersky E. 2005. Metabolic, genomic, and biochemical analyses of glandular trichomes from the wild tomato species *Lycopersicon hirsutum* identify a key enzyme in the biosynthesis of methylketones. The Plant Cell 17 (4): 1252–1267. DOI: https://doi.org/10.1105/tpc.104.029736

Gebrechristos H.Y., Chen W. 2018. Utilization of potato peel as eco-friendly products: A review. Food Science & Nutrition 6 (6): 1352–1356. DOI: https://doi.org/10.1002/fsn3.691

Hamilton J.P., Hansey C.N., Whitty B.R., Stoffel K., Massa A.N., Van Deynze A., De Jong W.S., Douches D.S., Buell C.R. 2011. Single nucleotide polymorphism discovery in elite north american potato germplasm. BMC Genomics 12 (1): 302. DOI: https://doi.org/10.1186/1471-2164-12-302

Isah T. 2019. Stress and defense responses in plant secondary metabolites production. Biological Research 52 (1): 39. DOI: https://doi.org/10.1186/s40659-019-0246-3

Jumper J.M., Evans R., Pritzel A., Green T., Figurnov M., Ronneberger O., Tunyasuvunakool K., Bates R., Žídek A., Potapenko A., Bridgland A., Meyer C., Kohl S.A., Ballard A., Cowie A., Romera-Paredes B., Nikolov S., Jain R., Adler J., Back T., Petersen S., Reiman D., Clancy E., Zielinski M., Steinegger M., Pacholska M., Berghammer T., Bodenstein S., Silver D., Vinyals O., Senior A.W., Kavukcuoglu K., Kohli P., Hassabis D. 2021. Highly accurate protein structure prediction with AlphaFold. Nature 596 (7873): 583–589. DOI: https://doi.org/10.1038/s41586-021-03819-2

Kalinger R.S., Pulsifer I.P., Rowland O. 2018. Elucidating the substrate specificities of acyl-lipid thioesterases from diverse plant taxa. Plant Physiology and Biochemistry 127: 104–118. DOI: https://doi.org/10.1016/j.plaphy.2018.03.013

Kennedy G.G., Yamamoto R.T., Dimock M.B., Williams W.G., Bordner J. 1981. Effect of day length and light intensity on 2-tridecanone levels and resistance in *Lycopersicon hirsutum* f. *glabratum* to *Manduca sexta*. Journal of Chemical Ecology 7 (4): 707–716. DOI: https://doi.org/10.1007/BF00990303

Khuat V.L.U., Bui V.T.T., Tran H.T.D., Truong N.X., Nguyen T.C., Mai P.H.H., Dang T.L.A., Dinh H.M., Pham H.T.A., Nguyen T.T.H. 2019. Characterization of *Solanum melongena* thioesterases related to tomato methylketone synthase 2. Genes 10 (7) DOI: https://doi.org/10.3390/genes10070549

Kornberg A., Ochoa S., Mehler A.H. 1948. Spectrophotometric studies on the decarboxylation of β-keto acids. The Journal of Biological Chemistry 174: 159–172.

Lenc L., Kwaśna H., Jeske M., Jończyk K., Sadowski C. 2016. Fungal pathogens and antagonists in root-soil zone in organic and integrated systems of potato production. Journal of Plant Protection Research 56 (2): 167–177. DOI: https://doi.org/10.1515/jppr-2016-0029

Li G., Zhou Y., Zhao Y., Liu Y., Ke Y., Jin X., Ma H. 2020. Internal reference gene selection for quantitative real-time RT-PCR normalization in potato tissues. Phyton 89 (2): 329–344. DOI: https://doi.org/10.32604/phyton.2020.08874

Lopez-Lara I.M., Nogales J., Pech-Canul A., Calatrava-Morales N., Bernabeu-Roda L.M., Duran P., Cuellar V., Olivares J., Alvarez L., Palenzuela-Bretones D., Romero M., Heeb S., Camara M., Geiger O., Soto M.J. 2018. 2-Tridecanone impacts surface-associated bacterial behaviours and hinders plant-bacteria interactions. Environmental Microbiology 20 (6): 2049–2065. DOI: https://doi.org/10.1111/1462-2920.14083

Maluf W.R., Barbosa L.V., Costa Santa-Cecília L.V. 1997. 2-Tridecanone-mediated mechanisms of resistance to the South American tomato pinworm *Scrobipalpuloides absoluta* (Meyrick, 1917) (Lepidoptera-Gelechiidae) in *Lycopersicon* spp. Euphytica 93 (2): 189–194. DOI: https://doi.org/10.1023/A:1002963623325

Massa A.N., Childs K.L., Lin H., Bryan G.J., Giuliano G., Buell C.R. 2011. The transcriptome of the reference potato genome *Solanum tuberosum* group Phureja clone DM1-3 516R44. PLoS ONE 6 (10): e26801. DOI: https://doi.org/10.1371/journal.pone.0026801

Mirdita M., Schütze K., Moriwaki Y., Heo L., Ovchinnikov S., Steinegger M. 2022. ColabFold: making protein folding accessible to all. Nature Methods 19 (6): 679–682. DOI: https://doi.org/10.1038/s41592-022-01488-1

Musetti L., Neal J.J. 1997. Toxicological effects of *Lycopersicon hirsutum* f. *glabratum* and behavioral response of *Macrosiphum euphorbiae*. Journal of Chemical Ecology 23 (5): 1321–1332. DOI: https://doi.org/10.1023/B:JOEC.0000006466.63606.0d

Nguyen L.-T., Schmidt H.A., von Haeseler A., Minh B.Q. 2015. IQ-TREE: A fast and effective stochastic algorithm for estimating maximum-likelihood phylogenies. Molecular Biology and Evolution 32 (1): 268–274. DOI: https://doi.org/10.1093/molbev/msu300

Paysan-Lafosse T., Blum M., Chuguransky S., Grego T., Pinto B.L., Salazar G.A., Bileschi M.L., Bork P., Bridge A., Colwell L., Gough J., Haft D.H., Letunić I., Marchler-Bauer A., Mi H., Natale D.A., Orengo C.A., Pandurangan A.P., Rivoire C., Sigrist C.J.A., Sillitoe I., Thanki N., Thomas P.D., Tosatto S.C.E., Wu C.H., Bateman A. 2023. InterPro in 2022. Nucleic Acids Research 51 (D1): 418–427. DOI: https://doi.org/10.1093/nar/gkac993

Pettersen E.F., Goddard T.D., Huang C.C., Meng E.C., Couch G.S., Croll T.I., Morris J.H., Ferrin T.E. 2021. <scp>UCSF ChimeraX</scp> : Structure visualization for researchers, educators, and developers. Protein Science 30 (1): 70–82. DOI: https://doi.org/10.1002/pro.3943

Pham G.M., Hamilton J.P., Wood J.C., Burke J.T., Zhao H., Vaillancourt B., Ou S., Jiang J., Buell C.R. 2020. Construction of a chromosome-scale long-read reference genome assembly for potato. GigaScience 9 (9) DOI: https://doi.org/10.1093/gigascience/giaa100

Van Poecke R.M.P., Posthumus M.A., Dicke M. 2001. Herbivore-induced volatile production by Arabidopsis thaliana leads to attraction of the parasitoid *Cotesia rubecula*: Chemical, behavioral, and gene-expression analysis. Journal of Chemical Ecology 27 (10): 1911–1928. DOI: https://doi.org/10.1023/A:1012213116515

Pulsifer I.P., Lowe C., Narayaran S.A., Busuttil A.S., Vishwanath A.J., Domergue F., Rowland O. 2014. Acyl-lipid thioesterase1-4 from Arabidopsis thaliana form a novel family of fatty acyl-acyl carrier protein thioesterases with divergent expression patterns and substrate specificities. Plant Molecular Biology 84 (4–5): 549–563. DOI: https://doi.org/10.1007/s11103-013-0151-z

Sattar F.A., Hamooh B.T., Wellman G., Ali M.A., Shah S.H., Anwar Y., Mousa M.A.A. 2021. Growth and biochemical responses of potato cultivars under *in vitro* lithium chloride and mannitol simulated salinity and drought stress. Plants 10 (5): 924. DOI: https://doi.org/10.3390/plants10050924

Tampe J., Parra L., Huaiquil K., Quiroz A. 2016. Potential repellent activity of the essential oil of *Ruta chalepensis* (linnaeus) from chile against *Aegorhinus superciliosus* (guérin) (Coleoptera: Curculionidae). Journal of Soil Science and Plant Nutrition DOI: https://doi.org/10.4067/S0718-95162016005000004

Tiwari J.K., Buckseth T., Zinta R., Bhatia N., Dalamu D., Naik S., Poonia A.K., Kardile H. B., Challam C., Singh R.K., Luthra S.K., Kumar V., Kumar M. 2022. Germplasm, breeding, and genomics in potato improvement of biotic and abiotic stresses tolerance. Frontiers in Plant Science 13 DOI: https://doi.org/10.3389/fpls.2022.805671

Tran H.T.D., Le N.T., Khuat V.L.U., Nguyen T.T.H. 2019. Identification and functional characterization of a soybean (*Glycine max*) thioesterase that acts on intermediates of fatty acid biosynthesis. Plants 8 (10): 397. DOI: https://doi.org/10.3390/plants8100397

Xu X., Pan S., Cheng S., Zhang B., Mu D., Ni P., Zhang G., Yang S., Li R., Wang J., Orjeda G., Guzman F., Torres M., Lozano R., Ponce O., Martínez D., De la Cruz G., Chakrabarti S.K., Patil V.U., Skryabin K.G., Kuznetsov B.B., Ravin N.V., Kolganova T.V., Beletsky A.V., Mardanov A.V., Di Genova A., Bolser D.M., Martin D.M., Li G., Yang Y., Kuang H., Hu Q., Xiong X., Bishop G.J., Sagredo B., Mejía N., Zagórski W., Gromadka R., Gawor J., Szczęsny P., Huang S., Zhang Z., Liang C., He J., Li Y., He Y., Xu J., Zhang Y., Xie B., Du Y., Qu D., Bonierbale M., Ghislain M., Herrera M.D., Giuliano G., Pietrella M., Perrotta G., Facella P., O'Brien K., Feingold S.E., Barreiro L.E., Massa G.A., Diambra L., Whitty B., Vaillancourt B., Lin H., Massa A.N., Geoffroy M., Lundback S., DellaPenna D., Buell C.R., Sharma S.K., Marshall D.F., Waugh R., Bryan G.J., Destefanis M., Nagy I., Milbourne D., Thomson S.J., Fiers M., Jacobs J.M., Nielsen K.L., Sønderkær M., Iovene M., Torres G.A., Jiang J., Veilleux R.E., Bachem C.W., de Boer J.M., Borm T.,

Kloosterman B., van Eck H.J., Datema E., Hekkert B.T., Goverse A., Van Ham R.C., Visser R. 2011. Genome sequence and analysis of the tuber crop potato. Nature 475 (7355): 189–195. DOI: https://doi.org/10.1038/nature10158

Xu G., Nguyen T.T., Guo Y., Schauvinhold I., Auldridge M.E., Bhuiyan N., Ben-Israel I., Iijima Y., Fridman E., Noel J.P., Pichersky E. 2010. Enzymatic functions of wild tomato methylketone synthases 1 and 2. Plant Physiology 154 (1): 67–77. DOI: https://doi.org/10.1104/pp.110.157073

Zhu J., Dhammi A., Kretschmar J.B., Vargo E.L., Apperson C.S., Michael Roe R. 2018. Novel use of aliphatic n-methyl ketones as a fumigant and alternative to methyl bromide for insect control. Pest Management Science 74 (3): 648–657. DOI: https://doi.org/10.1002/ps.4749